MICROSCOPIC STERN-GERLACH EFFECT AND THOMAS SPIN PRECESSION AS AN ORIGIN OF THE SSA

V.V. Abramov[1]

(1) *Institute for High Energy Physics, Protvino, Russia*
† *E-mail: Victor.Abramov@ihep.ru*

Abstract

The single-spin asymmetry and hadron polarization data are analyzed in the framework of a phenomenological effective-color-field model. Global analysis of the single-spin effects in hadron production is performed for h+h, h+A, A+A and lepton+N interactions. The model explains the dependence of the data on x_F, p_T, collision energy $\sqrt{s}$ and atomic weights A_1 and A_2 of colliding nuclei. The predictions are given for not yet explored kinematical regions.

In this report we discuss a semi-classical mechanism for the single-spin phenomena in inclusive reaction $A+B \to C+X$. The major assumptions of the model are listed below.

1) An effective color field (ECF) is a superposition of the QCD string fields, created by spectator quarks and antiquarks after the initial color exchange.

2) The constituent quark Q of the detected hadron C interacts with the nonuniform chromomagnetic field via its chromomagnetic moment $\mu^a_Q = s g^a_Q g_S/2M_Q$ and with the chromoelectric field via its color charge g_S.

3) The microscopic Stern-Gerlach effect in chromomagnetic field $\mathbf{B^a}$ and Thomas spin precession in chromoelectric field $\mathbf{E^a}$ lead to the large observed SSA. The ECF is considered as an external with respect to the quark Q of the observed hadron.

4) The quark spin precession in the ECF (chromomagnetic and chromoelectric) is an additional phenomenon, which leads to the specific SSA dependence (oscillation) as a function of kinematical variables (x_F, p_T or scaling variable $x_A = (x_R + x_F)/2$).

The longitudinal field $\mathbf{E^a}$ and the circular field $\mathbf{B^a}$ of the ECF are written as

$$E^{(3)}_Z = -2\alpha_s\nu_A/\rho^2 exp(-r^2/\rho^2)\,, \quad B^{(2)}_\varphi = -2\alpha_s\nu_A r/\rho^3 exp(-r^2/\rho^2)\,, \tag{1}$$

where r is the distance from the string axis, ν_A is the number of quarks at the end of the string, $\rho = 1.25R_c$, R_c - confinement radius, $\alpha_s \approx 1$ - running coupling constant [1,2].

The Stern-Gerlach type forces act on a quark moving inside the ECF (flux tube):

$$f_x = \mu^a_x \partial B^a_x/\partial x + \mu^a_y \partial B^a_y/\partial x\,, \quad f_y = \mu^a_x \partial B^a_x/\partial y + \mu^a_y \partial B^a_y/\partial y\,. \tag{2}$$

The quark Q of the observed hadron C, which gets p_T kick of Stern-Gerlach forces and undergo a spin precession in the ECF is called a "probe" and it "measures" the fields $\mathbf{B^a}$ and $\mathbf{E^a}$. The ECF is created by spectator quarks and antiquarks and obeys quark counting rules. Spectators are all quarks which are not constituents of the observed hadron C. In the case of $p^\uparrow + p \to \pi^+ + X$ reaction (see Fig. 1) polarized probe u quark from π^+ feels the field, created by the spectator quarks with weight $\lambda = -|\Psi_{qq'}(0)|^2/|\Psi_{q\bar{q}'}(0)|^2 \approx -1/8$, by antiquarks with weight 1, and by target quarks with weight $-\tau\lambda$, respectively. Spectator

quarks from the target B have an additional negative factor $-\tau = -0.0562 \pm 0.030$, since these quarks are moving in opposite direction in cm reference frame. The value of color factor $\lambda = -0.1321 \pm 0.0012$, obtained in a global fit of 68 inclusive reactions, is close to the expected one, which is a strong argument in favor of the ECF model [2].

Another important phenomenon is quark spin precession in the ECF. We assume that the spin precession is described by the Bargman-Michel-Telegdi eqs. (3)-(4) [3]:

$$d\xi/dt = a[\xi\mathbf{B^a}] + d[\xi[\mathbf{E^a v}]], \tag{3}$$

$$a = g_S(g_Q^a - 2 + 2M_Q/E_Q)/2M_Q\,, \quad d = g_S[g_Q^a - 2E_Q/(E_Q + M_Q)]/2M_Q\,. \tag{4}$$

The precession frequency depends on the color charge g_S, the quark mass M_Q and its energy E_Q, and on the color g_Q^a-factor. The value $\Delta\mu^a = (g_Q^a - 2)/2$ is called a color anomalous magnetic moment and it is large and negative in the instanton model. Spontaneous chiral symmetry breaking leads to an additional dynamical mass $\Delta M_Q(q)$ and $\Delta\mu^a(q)$, both depend on momentum transfer q [4]. Kochelev predicted $\Delta\mu^a(0) = -0.2$ [5] and Diakonov predicted $\Delta\mu^a(0) = -0.744$ [4]. The global data analysis results are closer to the Diakonov's predictions.

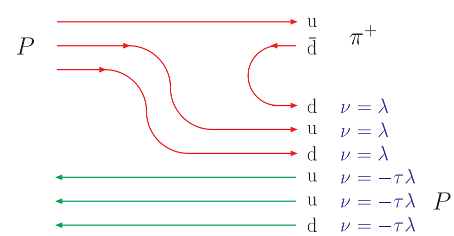

Figure 1: The quark flow diagram for the reaction $p^\uparrow + p \to \pi^+ + X$. The weight ν of each spectator quark contribution to the ECF is indicated.

Due to the microscopic Stern-Gerlach effect the probe quark Q gets an additional spin-dependent transverse momentum δp_x, which causes an azimuthal asymmetry or observed hadron polarization:

$$\delta p_x = \frac{g_Q^a \xi_y^0}{2\rho(g^a - 2 + 2M_Q/E_Q)}[\frac{1-\cos(\phi_A)}{\phi_A} + \epsilon\phi_A], \tag{5}$$

where $\phi_A = \omega_A x_A$ is a quark spin precession angle in the fragmentation region of the beam particle A, and a "frequency" of A_N oscillation as a function of x_A is

$$\omega_A = \frac{g_S \alpha_s \nu_A S_0 (g_Q^a - 2 + 2M_Q/E_Q)}{M_Q \rho^2 c}\,. \tag{6}$$

The length S_0 of the ECF is 0.6 ± 0.2 fm. The constituent quark masses M_Q and $\Delta\mu^a$ values are given in [2]. The parameter $\epsilon = -0.00419 \pm 0.00022$ is small due to subtraction of the Thomas precession term from $\epsilon = 1/2$ for chromomagnetic contribution to the δp_x.

Let us consider in more detail the Thomas precession effect in the ECF. Due to the Thomas precession an additional term $U = \mathbf{s} \cdot \omega_\mathbf{T}$ appears in the effective Hamiltonian. The Thomas frequency $\omega_\mathbf{T} \approx [\mathbf{Fv}]/M_Q$ depends on the force $\mathbf{F}$, the quark velocity $\mathbf{v}$ and its mass M_Q. The quark polarization due to the Thomas precession, $\delta\mathbf{P_N} = -\omega_\mathbf{T}/\Delta E$, is directed opposite to the frequency vector $\omega_\mathbf{T}$ direction since ΔE is positive [6].

The sign and magnitude of the force $\mathbf{F} = g_S\mathbf{E^a}$ is determined by the quark-counting rules for the ECF. For example, $F_Z \approx -2g_S\alpha_S[1 + \lambda - 3\tau\lambda]/\rho^2 < 0$ for the $pp \to \Lambda^\uparrow + X$ reaction at $\sqrt{s} < 70$ GeV. In case of the reactions $pp \to \Xi^{0\uparrow} + X$ and $p^\uparrow + p \to \pi^+ + X$ the factor in square brakets is $[2 + 2\lambda - 3\tau\lambda] < 0$ and $[3\lambda - 3\tau\lambda] > 0$, respectively.

Recombination potential is more attractive for negative $U = \mathbf{s} \cdot \omega_\mathbf{T}$. As a result, for the $pp \to \Lambda^\uparrow + X$ reaction the additional Thomas precession contribution to P_N is positive and opposite in sign to the dominating chromomagnetic term, which gives $P_N < 0$, and to the

DeGrand-Miettinen model predicted $P_N < 0$ [6]. The additional transverse momentum δp_x is related to the analyzing power or polarization by the relation $A_N = -D\delta p_x$, where $D = 5.68 \pm 0.13$ GeV^{-1} is an effective slope of the invariant cross section. In the Ryskin model $\delta p_x \approx 0.1$ GeV/c is a constant [7]. In the ECF model we have dynamical origin of A_N or P_N dependence on the kinematical variables (p_T, x_A, $x_B = (x_R - x_F)/2$, x_F) and on the number of (anti)quarks in hadrons A, B and C, and also on quark g_Q^a-factor and its mass M_Q. This dependence is due to the microscopic Stern-Gerlach effect and quark spin precession in the ECF [2].

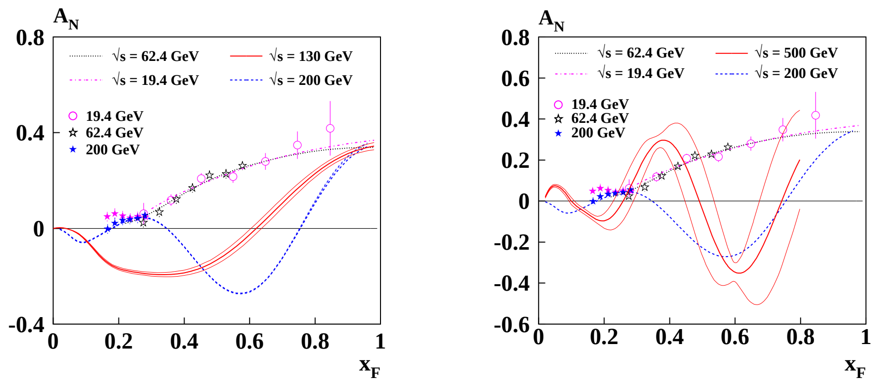

(a) **(b)**

Figure 2: The dependence $A_N(x_F)$ for $p^\uparrow + p \to \pi^+ + X$ reaction. Predictions are for **(a)** $\sqrt{s} = 130$ GeV and **(b)** $\sqrt{s} = 500$ GeV, respectively. The cm production angle is 4.1^o.

The ECF increases dramatically at energy $\sqrt{s} > 70$ GeV or in collisions of nuclei. In the case of nuclei collisions the effective number of quarks in a projectile nuclei, which contributes to the ECF, is equal to its number in a tube with transverse radius limited by the confinement. The new quark contribution to the ECF depends on kinematical variables:

$$f_N = n_q \exp(-W/\sqrt{s})(1 - x_N)^n \,, \quad x_N = [(p_T/p_N)^2 + x_F^2]^{1/2} \,, \tag{7}$$

where $W \approx 238(A_1A_2)^{-1/6}$ GeV, $n \approx 0.91(A_1A_2)^{1/6}$, $p_N \approx 28$ GeV/c and $n_q \approx 4.52$ [2].

Due to the dependence of the ECF on $\sqrt{s}$ and atomic weights A_1, A_2 of colliding particles we expect very unusual behavior of A_N and P_N as a function of kinematical variables. The data and model predictions of A_N for the π^+ production in pp-collisions are shown in Fig. 2a as a function of x_F. The data are from the E704 [8] and BRAHMS [9] experiments for cm energies 19, 62 and 200 GeV. The model predictions describe the data. The dashed curve is for 200 GeV and the solid curve is for 130 GeV. We expect a negative A_N for 200 GeV and x_F around 0.6 and also for 130 GeV and x_F in the range from 0.1 to 0.6. The negative A_N values are due to the u-quark spin precession in a strong ECF. Even more unusual oscillating behavior of A_N is expected for 500 GeV (see Fig. 2b).

In Fig. 3 the global polarization P_N of Λ hyperon in Au+Au collisions is shown as a function of p_T. The data are from STAR experiment at 62 and 200 GeV [10]. The ECF model predictions reproduce the data. Oscillating behavior of P_N is due to the s-quark spin precession in very strong color fields. Similar oscillating behavior of P_N, as a function of pseudorapidity, is expected for low energies, 7 and 9 GeV in cm. The predictions are shown in Fig. 4 for S+S, Cu+Cu, and Au+Au collisions, respectively.

Conclusion: a semi-classical mechanism is proposed for single-spin phenomena. The effective color field of QCD strings, created by spectator quarks and antiquarks is described by the quark-counting rules. The microscopic Stern-Gerlach effect in the chromomagnetic field and the Thomas spin precession in the chromoelectric field lead to the SSA. The energy and atomic weight dependence of the effective color fields, combined with the quark spin precession phenomenon, lead to the oscillating behavior of A_N and P_N. The model predictions for different reactions and energies can be checked at the existing accelerators.

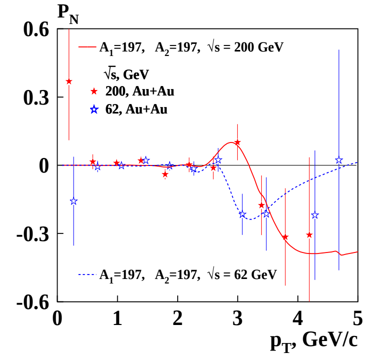

Figure 3: The dependence $P_N(p_T)$ of Λ-hyperon polarization in Au+Au collisions.

References

[1] A.B. Migdal and S.B. Khokhlachev, JETP Lett. **41** (1985) 194.

[2] V.V. Abramov, Yad. Fiz. **72** (2009) 1933 [Phys. At. Nucl. **72** (2009) 1872].

[3] V. Bargmann, L. Michel and V. Telegdy, Phys. Rev. Lett. **2** (1959) 435.

[4] D. Diakonov, Prog. Part. Nucl. Phys. **51** (2003) 173.

[5] N.I. Kochelev, Phys. Lett. **B426** (1998) 149.

[6] T.A. DeGrand, H.I. Miettinen, Phys. Rev. **D24** (1981) 2419.

[7] M.G. Ryskin, Yad. Fiz. **48** (1988) 1114 [Sov. J. Nucl. Phys. **48** (1988) 708].

[8] D.L. Adams et al., Phys. Lett. **B264** (1991) 462.

[9] J.H. Lee and F. Videbaek (BRAHMS Collab.), AIP Conf. Proc. **915** (2007) 533.

[10] B.I. Abelev et al., Phys. Rev. **C76** (2007) 024915.

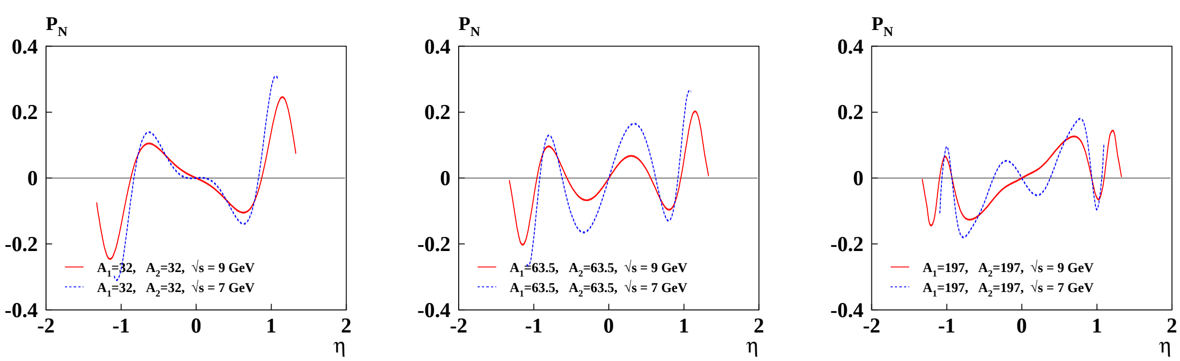

(a) **(b)** **(c)**

Figure 4: The transverse polarization of Λ vs $\eta = -ln(\tan\theta_{CM}/2)$ at $p_T = 2.35$ GeV/c in **(a)** S+S, **(b)** Cu+Cu and **(c)** Au+Au collisions. Solid line corresponds to $\sqrt{s} = 9$ GeV and dashed line to $\sqrt{s} = 7$ GeV, respectively.